

DISENTANGLING THE SPATIAL STRUCTURE AND STYLE IN CONDITIONAL VAE

Ziye Zhang, Li Sun, Zhilin Zheng and Qingli Li

Shanghai Key Laboratory of Multidimensional Information Processing,
Key Laboratory of Advanced Theory and Application in Statistics and Data Science
East China Normal University, 200241 Shanghai, China

ABSTRACT

This paper aims to disentangle the latent space in cVAE into the spatial structure and the style code, which are complementary to each other, with one of them z_s being label relevant and the other z_u irrelevant. The generator is built by a connected encoder-decoder and a label condition mapping network. Depending on whether the label is related with the spatial structure, the output z_s from the condition mapping network is used either as a style code or a spatial structure code. The encoder provides the label irrelevant posterior from which z_u is sampled. The decoder employs z_s and z_u in each layer by adaptive normalization like SPADE or AdaIN. Extensive experiments on two datasets with different types of labels show the effectiveness of our method.

Index Terms— cVAE, GAN, disentanglement

1. INTRODUCTION

VAE [1] and GAN [2] are two powerful tools for image synthesis. In GAN, the generator $G(z)$ aims to mimic the data distribution $p_{\text{data}}(x)$ with an approximation $p_G(z)$ by mapping the random noise z drawn from prior to the image-like data. Meanwhile, GAN learns a discriminator D to distinguish the source of samples, either drawn from $p_{\text{data}}(\mathbf{x})$ or $p_G(z)$. G and D are trained jointly in an adversarial manner. VAE consists of a pair of connected encoder and decoder. The encoder $q_\phi(z|x)$ maps the data x into a code z , and decoder $p_\theta(x|z)$ transforms z into image domain and tries to reconstruct x . $q_\phi(z|x)$ to be simple, *e.g.*, close to the standard Gaussian prior $N(0, \mathbf{I})$ based on the KL divergence metric.

Compared to GAN, VAE tends to generate blurry images, since $q_\phi(z|x)$ is too simple to capture the true posterior, known as "posterior collapse". But it is easier to train. While GAN's optimization is unstable, hence many works try to stabilize its training [3–5]. Moreover, VAE explicitly models each dimension of z as independent Gaussian, so it can disentangle the factors in unsupervised way [6, 7]. To fully exploit the advantage from both of them, VAE and GAN can be combined into VAE-GAN [8], in which the encoder and decoder in VAE forms the generator, and it employs a discriminator to identify the real from the fake image including

the reconstructed and the prior sampling image.

Both GAN and VAE can be utilized for conditional generation. The generator in conditional GAN (cGAN) [9, 10] is usually given the concatenation of a random code z and a conditional label c . Its output $G(z, c)$ is required to fulfill the condition. Here c has various forms. It can be a one-hot vector indicating the categories, or an conditional image with its spatial structure. D in cGAN not only evaluates the reality of $G(z, c)$, but also checks its conformity on c . Similarly, cVAE [11] is provided with the label c to both encoder and decoder. The posterior specified by the encoder becomes $q_\phi(z|x, c)$. Note that x with different c are mapping to the same prior $N(0, \mathbf{I})$, so the regularization term actually prevents z being relevant with c . Then the decoder $p_\theta(x|z, c)$ reconstructs x by concatenate c with z . Like VAE-GAN [8], cVAE can also be extended to cVAE-GAN introduced in [12].

In cVAE, the label relevant and irrelevant factors are all included in the posterior $q_\phi(z|x, c)$, hence manipulating $z \sim q_\phi(z|x, c)$ often leads to the unnecessary change on the given condition. Moreover, the synthesized images in cVAE often have the low conformity on the condition. To improve the conditional synthesized results, some works try to disentangle label relevant factors from all the others. CSVAE [13] proposes to learn the conditional label relevant subspace by using distinct priors under the different labels. Zheng *et al.* [14] employs two encoders. One learns the label dependent priors and specifies the posterior z_s as a δ function. The other uses a $N(0, \mathbf{I})$ Gaussian prior, and maps the data into a label irrelevant posterior $q_\phi(z_u|x)$. Both the works adopt the adversarial training to prevent z_u from carrying the label information.

This paper also focuses on disentangling the label relevant and irrelevant factors in cVAE. Different from previous works, we model the label irrelevant posterior based on the same prior, and treat the label relevant factors a deterministic code. Moreover, our method does not apply the adversarial training to minimize the mutual information between the label and its irrelevant factors, which makes the optimization easy. The key idea is to employ a spatial preserving posterior and a style code, or vice versa, a style posterior and a spatial structure code to synthesize the image. Note that the two cases actually correspond to different structures in cVAE. They are chosen depending on whether the label condition is

spatial related or not, and posteriors in both of them are constrained in the same way, close to the prior $N(0, \mathbf{I})$, thus the code sampling from it is label irrelevant. Particularly, the spatial structure code, either sampling from the posterior or mapping from the label, is applied into the encoder and decoder through spatially-adaptive normalization (SPADE) [15]. On the other hand, the style code is incorporated into VAE by adaptive instance normalization (AdaIN) [16,17]. To improve the quality of the synthesis, we add a discriminator like cVAE-GAN [12], and extend the fake data.

Our contribution lies in following aspect. First, we propose a simple, flexible method to disentangle the spatial structure and style code for image synthesis. We only require one of them is label dependent, and it is given to the generator as the condition. The other is fully unsupervised and becomes label irrelevant after training. Second, by applying the adaptive normalization based on both the style and the spatial structure code, our model improves the disentangling performance. We carry out experiments on two types of datasets to prove the effectiveness of the method.

2. PROPOSED METHOD

We now give the details about the proposed method. Fig.1 shows the overall architecture. The generator G consists of Enc , Dec and a small condition mapping network f . Enc specifies the spatial structure preserving posterior $N(\mu, \sigma)$ which is assumed to be label irrelevant, and constrained with prior $N(0, \mathbf{I})$ by KL divergence. Dec exploits the spatial structure code $z_u \sim N(\mu, \sigma)$ with SPADE, and the style code w given by f with AdaIN. The connected Enc and Dec are trained by the reconstruction loss L_{rec} . The discriminator D helps G synthesizing the high quality image by providing the adversarial GAN loss $L_{D/G}^{adv}$.

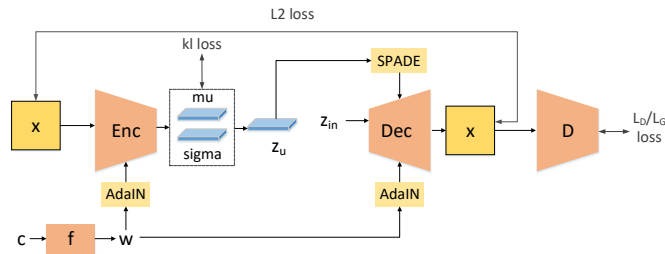


Fig. 1. The proposed architecture on FaceScrub, in which ID labels have few spatial cues, and they are mapped into style codes. Dec exploits the spatial structure code $z_u \sim N(\mu, \sigma)$ with SPADE, and the style code w given by f with AdaIN. Note that the best architecture is different on 3D chair.

2.1. Problem formulation

Supposing the image is x and its label is c , the goal of cVAE is to maximize the ELBO defined in (1), so that the data

log-likelihood $\log p(x)$ can be maximized. As is described in [14], the key idea is to split the latent code z into separate codes, the label relevant z_s and irrelevant z_u . Here ϕ , ψ and θ , correspond to the model parameters in Enc , Dec and f , respectively. D_{KL} indicates the KL divergence between two distributions. Note that there are three terms in (1). The first one is the negative reconstruction error. The second and third terms are the regularization which pushes the $q_\phi(z_u|x, c)$ and $q_\psi(z_s|c)$ to their priors $p(z_u)$ and $p(z_s)$, respectively. In practice, we assume that z_s is deterministic, which means $p(z_s)$ and $q_\psi(z_s|c)$ are both dirac δ function. Hence the third term is strictly required to be 0, thus can be ignored.

$$\begin{aligned} \log p(x) \geq & \mathbb{E}_{q_\phi(z_u|x), q_\psi(z_s|x)} [\log p_\theta(x|z_u, z_s)] \\ & - D_{KL}(q_\phi(z_u|x, c) || p(z_u)) \\ & - D_{KL}(q_\psi(z_s|c) || p(z_s)) \end{aligned} \quad (1)$$

2.2. Details about the network

2.2.1. Conditional label mapping network f

As is illustrated in Fig. 1, The input of f is a conditional label c , which indicates the category of x , usually expressed in one-hot format. Like [17], we first use several fully-connected layers to map c into an embedding code w , which is later used by both the Enc and Dec based on the adaptive normalization module. Here the output w is regarded as the label relevant code z_s in (1) which is $w = z_s$, and it is treated either as a spatial structure preserving feature map with its dimension $H \times W \times 1$, or a style feature with its size $1 \times 1 \times C$. We make the choice based on whether c is directly related with the spatial structure. Actually, we try both cases on two different datasets, 3D chair [18] and FaceScrub [19]. The details are given in the experiments section.

2.2.2. Encoder and Decoder

cVAE has a pair of connected Enc and Dec . The Enc takes the image and label pair x, c and maps it into a posterior probability, which is assumed to have the Gaussian form $p(z_u|x, c) = N(z_u|x, c; \mu, \sigma)$. Here μ and σ are the mean and standard deviation, which are two outputs from Enc depending on x . A code $z_u \sim p(z_u|x, c)$ is sampled from it to synthesize the reconstruction of x . Note that in VAE, there is a prior assumption on z_u , which is $p(z_u) = N(z_u; 0, \mathbf{I})$. During the optimization, $D_{KL}(p(z_u|x, c) || p(z_u))$ is considered. In other words, the Enc tries to map x from various classes into the same prior. Therefore z_u tends to be label irrelevant in cVAE.

In our scheme, we also have two choices on the output of the Enc , which are closely related to output z_s (or w) from the condition mapping network f . Particularly, z_u can be assumed as either a spatial structure code with its size $H \times W \times 1$ or a style code with the dimension $1 \times 1 \times C$. In the first case, the spatial structure is kept from x so there should be no fully-connected layers in the Enc . In the second case, z_u is

formulated to capture the feature channel style based on the global average pooling. To make z_u complementary to z_s , we intentionally design it so that one of z_u or z_s is the style code and the other is the spatial structure code. In the experiments, we demonstrate that different dimension settings for z_s and z_u improve disentangling performances.

The *Dec* takes the code z_s and z_u and tries to reconstruct x . Traditionally, all inputs are directly concatenated in the channel dimension, then fed into the *Dec* as its input. However, this simple strategy dose not emphasize the difference between z_s and z_u , which definitely degrades the disentangling quality. Inspired by two adaptive normalization structure, AdaIN [17] and SPADE [15], we find they are suitable for our task. As is shown in (2), $h^{(l)} \in \mathbb{R}^{N,C,H,W}$ is an activation map in l th layer of *Dec*, and $\hat{h}^{(l)}$ is the tensor after the normalization. γ, β are two outputs from the conditional branch, depending on z_s or z_u . μ_h and σ_h are the mean and standard deviation statistics on $h^{(l)}$. SPADE and AdaIN have different strategies to manipulate μ_h, σ_h, β and γ . In SPADE, μ_h and σ_h are computed on H, W and N , while β, γ are provided with distinct values along C, H and W . In AdaIN, the statistics are computed on H and W , and it only specifies β and γ along the channel dimension C . Our method uses SPADE and AdaIN for processing the spatial structure and style code, respectively. $h^{(l)}$ is processed by SPADE and AdaIN at the same time. Then we concatenate the results and reduce the channel dimensions through 1×1 conv.

$$\hat{h}^{(l)} = \gamma \frac{h^{(l)} - \mu_h}{\sigma_h} + \beta \quad (2)$$

2.2.3. Discriminator

Traditional cVAE has only a pair of *Enc* and *Dec*. Thus they are optimized only by the reconstruction loss with a KL divergence as a regularization like (1). To improve the synthesis and disentangling quality, we add adversarial training by employing a discriminator D with its parameters θ_D to inspect the quality of fake data. This extra D gives another benefit, that we can have more types of fake data since D evaluate them. In [8, 12], the prior sampling image with $z_u \sim N(0, I)$ is given to D . Our work extend it by synthesizing the exchanged image with z_s and z_u coming from different image. Note that D proposed in [10] used in our work. The score of D ranges from -1 to 1. The adversarial training loss for discriminator is in (3). Here the first term reflects the score for real image, and the other three terms are the scores for the reconstructed, exchanged and prior sampled image.

$$\begin{aligned} L_D^{adv} = & \mathbb{E}_{x \sim p_{\text{data}}} [\max(0, 1 - D(x, c))] \\ & + \mathbb{E}_{z_u \sim N(\mu, \sigma)} [\max(0, 1 + D(\text{Dec}(z_u, z_s(c))), c)] \\ & + \mathbb{E}_{z_u \sim N(\mu, \sigma)} [\max(0, 1 + D(\text{Dec}(z_u, z_s(c')), c')] \\ & + \mathbb{E}_{z_u \sim N(0, I)} [\max(0, 1 + D(\text{Dec}(z_u, z_s(c))), c)] \end{aligned} \quad (3)$$

3. EXPERIMENTS

3.1. Experimental Setup

Datasets. We conduct experiments on two datasets, including the 3D chair [18] and the FaceScrub [19]. The 3D chair depicts a wide variety of chairs in 62 different chosen azimuth angles. Images are resized to the fixed size 64×64 . The Facescrub contains 107k facial images from 530 different IDs. These faces are cropped by the detectors [20], and they are aligned based on the facial landmarks [21]. The detected cropped images are in 128×128 .

Evaluation metrics. We adopt three metrics for quantitative analysis. (1) Classification Accuracy (*Acc*) reflects the condition conformity of the generated images. We use models of ResNet-50 [22] trained on these two datasets for evaluating. (2) Fréchet Inception Distance (*FID*) [23] measures the distance between distributions of the synthesized and the real images, thus the lower, the better. (3) Mutual Information (*MI*) between label irrelevant code z_u and original label c . If label relevant and irrelevant variables are disentangled well, the mutual information value $I(z_u; c)$ should be small:

$$\begin{aligned} I(z_u; c) &= \mathbb{E}_{q(z_u|c)p(c)} \log \frac{q(z_u|c)}{q(z_u)} \\ &= \frac{1}{C} \sum_c \mathbb{E}_{q(z_u|c)} \log \frac{q(z_u|c)}{q(z_u)} \end{aligned} \quad (4)$$

$q(z_u|c)$ and $q(z_u)$ are hard to be computed directly, but can be approximated with Monte Carlo simulation.

3.2. Results

3D chair. The label of 3D chair is azimuth angle. The model can generate chair with the specified azimuth, and the output image should preserve original chair style. Here, the spatial structure code is label relevant and the style code irrelevant. Different from Fig.1, *Dec* adopts the style code $z_u \sim N(\mu, \sigma)$ with AdaIN, and the spatial code z_s with SPADE.

We compare our method with cVAE-GAN, and other four models for ablation study. The first model S1 makes a simple change on cVAE-GAN, incorporates label condition into *Enc* and *Dec* by exploiting label relevant code z_s with AdaIN. S2 uses SPADE to process z_s which is reshaped to $H \times W \times 1$. S3 is similar with our proposed structure except the embedding code z_s is applied with AdaIN. S4 manipulates spatial structure code z_s with AdaIN, and style code z_u with SPADE.

Facescrub. Facescrub provides ID labels. The model is supposed to output facial image with specified ID but preserve label irrelevant information, like pose, expression, from the input image. It is obviously that the label relevant code controls the style and the label irrelevant code specifies spatial related information. Fig.1 shows our proposed method. Also, we compare our method with cVAE-GAN, and choose S1 and S3 described previously for ablation study.

Table 1. The comparison network structures on two datasets. For z_s , two choices are AdaIN and SPADE. For z_u , it can also given to *Dec* directly. Note that we do not list and compare all possible ways. But these are typical ones.

		3D chair					Facescrub		
z_s	cVAE-GAN	S1	S2	S3	S4	Proposed	S1	S3	Proposed
	concat	AdaIN	SPADE	AdaIN	AdaIN	SPADE	AdaIN	AdaIN	AdaIN
z_u	<i>Dec</i> input	<i>Dec</i> input	<i>Dec</i> input	AdaIN	SPADE	AdaIN	<i>Dec</i> input	AdaIN	SPADE

Table 1 lists the comparison structures in our experiments on two datasets. “*Dec* inputs” indicates that the code is taken as *Dec*’s input. “AdaIN” or “SPADE” means the corresponding code is incorporated into *Dec* by this operation.

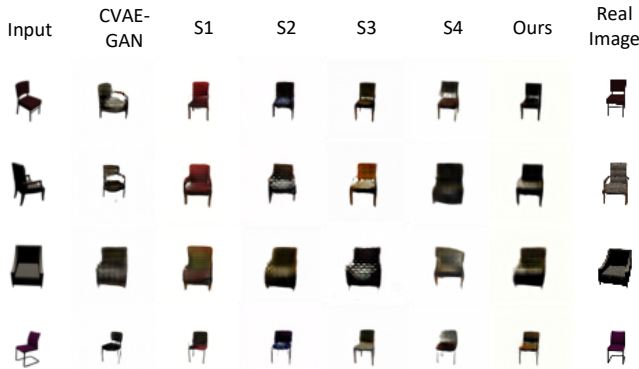


Fig. 2. Exchanged images on 3D chair are shown here.

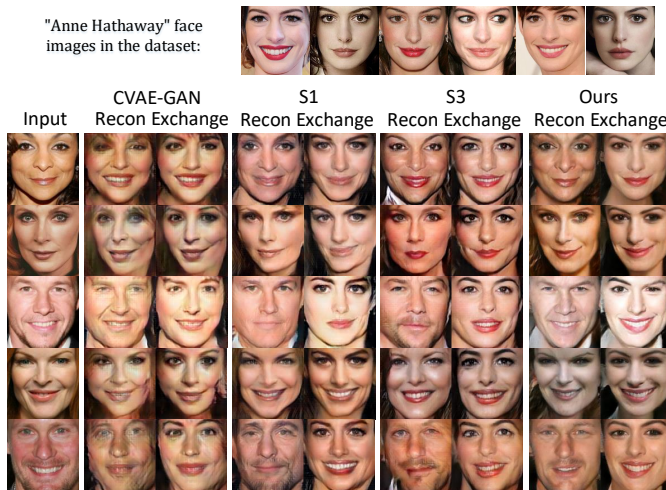


Fig. 3. Reconstructed and exchanged images on FaceScrub.

3.3. Analysis

We choose one specific label to generate images. All the images we analyze here are exchanged images. For 3D chair, the input label is “24” and for Facescrub the label is “Anne

Table 2. *MI* and *Acc* on 3D chair from different models.

	<i>MI</i>	<i>Acc</i>
cVAE-GAN	3.777	0.124
S1	3.773	0.573
S2	3.765	0.608
S3	3.775	0.511
S4	3.774	0.404
Proposed method	3.750	0.623

Table 3. *Acc* and *FID* on Facescrub from different models.

	<i>Acc</i>	<i>FID</i>
cVAE-GAN	0.072	83.05
S1	0.444	80.37
S3	0.498	52.46
Proposed method	0.632	50.14

Hathaway”. The generated images from different models on 3D chair and Facescrub are presented in Fig.2 and Fig.3, respectively. In both Fig.2 and Fig.3, images generated from our proposed method achieves the best performance.

To validate the proposed model, we compute the *MI* in (4) and *Acc* on 3D chair, and the *Acc* and *FID* score on Facescrub. Results are shown in Table 2 and Table 3. For *MI* and *Acc*, we generate 100 images for each label. For *FID* score, due to the Facescrub has a large number of labels, we choose 5 identities for evaluation. Each identity has 5000 images and we calculate the average *FID* on the chosen 5 categories. As shown in Table 2 and Table 3, our proposed method which uses SPADE and AdaIN to process the spatial structure and style code respectively, achieves the best score on both datasets.

4. CONCLUSION

We propose a latent space disentangling algorithm for conditional image synthesis in cVAE. Our method divides the latent code into label relevant and irrelevant parts. One of them preserves the spatial structure, and the other is the style code. These two types of codes are applied into cVAE by different adaptive normalization schemes. Together with a discriminator in the pixel domain, our model can generate high quality images, and achieve the disentangling performance.

5. REFERENCES

- [1] Danilo Jimenez Rezende, Shakir Mohamed, and Daan Wierstra, “Stochastic backpropagation and approximate inference in deep generative models,” *arXiv preprint arXiv:1401.4082*, 2014.
- [2] Ian Goodfellow, Jean Pouget-Abadie, Mehdi Mirza, Bing Xu, David Warde-Farley, Sherjil Ozair, Aaron Courville, and Yoshua Bengio, “Generative adversarial nets,” in *Advances in neural information processing systems*, 2014, pp. 2672–2680.
- [3] Martin Arjovsky, Soumith Chintala, and Léon Bottou, “Wasserstein generative adversarial networks,” in *International Conference on Machine Learning*, 2017, pp. 214–223.
- [4] Ishaan Gulrajani, Faruk Ahmed, Martin Arjovsky, Vincent Dumoulin, and Aaron C Courville, “Improved training of wasserstein gans,” in *Advances in Neural Information Processing Systems*, 2017, pp. 5767–5777.
- [5] Takeru Miyato, Toshiki Kataoka, Masanori Koyama, and Yuichi Yoshida, “Spectral normalization for generative adversarial networks,” *arXiv preprint arXiv:1802.05957*, 2018.
- [6] Irina Higgins, Loic Matthey, Arka Pal, Christopher Burgess, Xavier Glorot, Matthew Botvinick, Shakir Mohamed, and Alexander Lerchner, “beta-vae: Learning basic visual concepts with a constrained variational framework.,” *ICLR*, vol. 2, no. 5, pp. 6, 2017.
- [7] Tian Qi Chen, Xuechen Li, Roger B Grosse, and David K Duvenaud, “Isolating sources of disentanglement in variational autoencoders,” in *Advances in Neural Information Processing Systems*, 2018, pp. 2610–2620.
- [8] Anders Boesen Lindbo Larsen, Søren Kaae Sønderby, Hugo Larochelle, and Ole Winther, “Autoencoding beyond pixels using a learned similarity metric,” *arXiv preprint arXiv:1512.09300*, 2015.
- [9] Mehdi Mirza and Simon Osindero, “Conditional generative adversarial nets,” *arXiv preprint arXiv:1411.1784*, 2014.
- [10] Takeru Miyato and Masanori Koyama, “cgans with projection discriminator,” *arXiv preprint arXiv:1802.05637*, 2018.
- [11] Kihyuk Sohn, Honglak Lee, and Xinchen Yan, “Learning structured output representation using deep conditional generative models,” in *Advances in neural information processing systems*, 2015, pp. 3483–3491.
- [12] Jianmin Bao, Dong Chen, Fang Wen, Houqiang Li, and Gang Hua, “Cvae-gan: fine-grained image generation through asymmetric training,” in *Proceedings of the IEEE International Conference on Computer Vision*, 2017, pp. 2745–2754.
- [13] Jack Klys, Jake Snell, and Richard Zemel, “Learning latent subspaces in variational autoencoders,” in *Advances in Neural Information Processing Systems*, 2018, pp. 6444–6454.
- [14] Zhilin Zheng and Li Sun, “Disentangling latent space forvae by label relevant/irrelevant dimensions,” in *Proceedings of the IEEE Conference on Computer Vision and Pattern Recognition*, 2019, pp. 12192–12201.
- [15] Taesung Park, Ming-Yu Liu, Ting-Chun Wang, and Jun-Yan Zhu, “Semantic image synthesis with spatially-adaptive normalization,” in *Proceedings of the IEEE Conference on Computer Vision and Pattern Recognition*, 2019, pp. 2337–2346.
- [16] Xun Huang and Serge Belongie, “Arbitrary style transfer in real-time with adaptive instance normalization,” in *Proceedings of the IEEE International Conference on Computer Vision*, 2017, pp. 1501–1510.
- [17] Tero Karras, Samuli Laine, and Timo Aila, “A style-based generator architecture for generative adversarial networks,” in *Proceedings of the IEEE Conference on Computer Vision and Pattern Recognition*, 2019, pp. 4401–4410.
- [18] Mathieu Aubry, Daniel Maturana, Alexei A Efros, Bryan C Russell, and Josef Sivic, “Seeing 3d chairs: exemplar part-based 2d-3d alignment using a large dataset of cad models,” in *Proceedings of the IEEE conference on computer vision and pattern recognition*, 2014, pp. 3762–3769.
- [19] Hong-Wei Ng and Stefan Winkler, “A data-driven approach to cleaning large face datasets,” in *2014 IEEE International Conference on Image Processing (ICIP)*. IEEE, 2014, pp. 343–347.
- [20] Dong Chen, Shaoqing Ren, Yichen Wei, Xudong Cao, and Jian Sun, “Joint cascade face detection and alignment,” in *European Conference on Computer Vision*. Springer, 2014, pp. 109–122.
- [21] Xuehan Xiong and Fernando De la Torre, “Supervised descent method and its applications to face alignment,” in *Proceedings of the IEEE conference on computer vision and pattern recognition*, 2013, pp. 532–539.
- [22] Kaiming He, Xiangyu Zhang, Shaoqing Ren, and Jian Sun, “Deep residual learning for image recognition,” in *Proceedings of the IEEE conference on computer vision and pattern recognition*, 2016, pp. 770–778.
- [23] Martin Heusel, Hubert Ramsauer, Thomas Unterthiner, Bernhard Nessler, and Sepp Hochreiter, “Gans trained by a two time-scale update rule converge to a local nash equilibrium,” in *Advances in Neural Information Processing Systems*, 2017, pp. 6626–6637.